

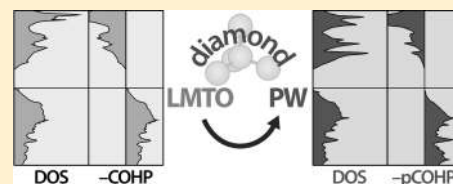
Crystal Orbital Hamilton Population (COHP) Analysis As Projected from Plane-Wave Basis Sets

Volker L. Deringer,[†] Andrei L. Tchougréeff,^{†,‡} and Richard Dronskowski^{*,†}

[†]Institute of Inorganic Chemistry, RWTH Aachen University, Landoltweg 1, D-52056 Aachen, Germany

[‡]Poncelet Laboratory, Moscow Center for Continuous Mathematical Education, Independent University of Moscow, Bolshoi Vlasevsky Per. 11, 119002 Moscow, Russia

ABSTRACT: Simple, yet predictive bonding models are essential achievements of chemistry. In the solid state, in particular, they often appear in the form of visual bonding indicators. Because the latter require the crystal orbitals to be constructed from local basis sets, the application of the most popular density-functional theory codes (namely, those based on plane waves and pseudopotentials) appears as being ill-fitted to retrieve the chemical bonding information. In this paper, we describe a way to *re-extract* Hamilton-weighted populations from plane-wave electronic-structure calculations to develop a tool analogous to the familiar crystal orbital Hamilton population (COHP) method. We derive the new technique, dubbed “projected COHP” (pCOHP), and demonstrate its viability using examples of covalent, ionic, and metallic crystals (diamond, GaAs, CsCl, and Na). For the first time, this chemical bonding information is *directly* extracted from the results of plane-wave calculations.



I. INTRODUCTION

There is a flourishing symbiosis between theoretical chemistry and physics when it comes to treating the solid state. In the 21st century, *ab initio* calculations not only guarantee a thorough understanding of existing phenomena but are also of tremendous help in the prediction of fascinating new materials. One of the cornerstones of *chemical* theory, however, has always been the quest for simple, yet powerful models that can be easily visualized,¹ and such models are particularly valuable when dealing with extended, three-dimensional structures, i.e., crystals. Here, the quantum-mechanical information is typically expressed in reciprocal space, which often poses a serious problem for both chemical intuition and imagination.

To overcome such difficulties in the framework of density-functional theory (DFT), the crystal orbital Hamilton population (COHP) analysis was introduced in 1993,² a DFT successor of the familiar crystal orbital overlap population (COOP) concept³ based on extended Hückel theory.⁴ COHP is a partitioning of the band-structure energy in terms of orbital-pair contributions, and it is therefore based on a local basis (the so-called tight-binding approach) as is commonly used in chemistry and parts of physics as well. Given that the interaction between two orbitals (say, the μ th and ν th one), centered at neighboring atoms, is described by their Hamiltonian matrix element $H_{\mu\nu} = \langle \phi_\mu | \hat{H} | \phi_\nu \rangle$, the multiplication with the corresponding densities-of-states matrix then easily serves as a quantitative measure of bonding strength because the product either lowers (bonding) or raises (antibonding) the band-structure energy. Thus, energy-resolved COHP(E) plots make bonding, nonbonding (no energetic effect), and antibonding contributions discernible at first glance, just like the earlier COOP(E) plots. Accordingly, COHP analysis has successfully answered numerous questions and furthermore made useful

predictions in the “chemical” language of local, atom-centered orbitals⁵ together with the underlying density-functional theory.

Physics, on the other hand, has been following alternative pathways. Bloch’s theorem⁶ suggests handling periodic systems quite differently, and the wave functions of the crystal are easily constructed in terms of plane waves that form an orthonormal and, in principle, complete description of the Hilbert space. In fact, plane waves appear as a natural (yet *highly* nonchemical!) choice for any crystalline system, and the price paid is obvious from the fact that the atomic nature of the material at hand is hidden in a plane-wave expansion; in addition, the atom’s nodal structure is totally removed by a numerically tractable pseudopotential ansatz. Today, an abundance of plane-wave electronic-structure codes is available,⁷ and plane-wave calculations have become the method of choice for fast, yet reliable theoretical materials science.⁸

To nonetheless apply chemical thinking, a couple of attempts have been carried out to reconstruct local quantities such as Mulliken charges from the results of plane-wave calculations. Already in 1995, Sánchez-Portal et al. introduced a projection technique⁹ that enabled studies on a broad range of different solids;¹⁰ the idea is similar to the one presented in this work. To date, however, no attempts have been made public for re-formulating a COHP-like quantity as well. Given that such a method exists, insightful chemical models will be available even when relying upon nonchemical computational approaches, namely the state-of-the-art plane-wave codes.

This paper is organized as follows. In section II, we describe the underlying theory and then develop the technique which we

Received: March 16, 2011

Revised: April 21, 2011

Published: May 06, 2011

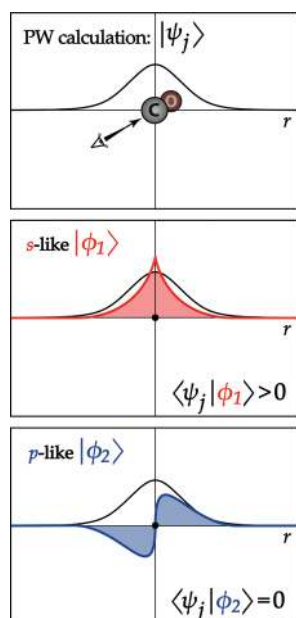


Figure 1. Schematic illustration of the projection technique from band function $|\psi_j\rangle$, taken from a periodic VASP calculation of the CO molecule, to local orbital $|\phi_\mu\rangle$. The band function (drawn in black, top) resembles a carbon 2s orbital and overlaps with the s-like local function $|\phi_1\rangle$ (middle). Its overlap with the p-like function $|\phi_2\rangle$, however, is zero due to orthogonality (bottom).

dub “projected COHP” (pCOHP); furthermore, details of all calculations are given. In section III, we describe applications of the new method to well-known covalent, ionic, and metallic model systems: diamond, gallium arsenide, cesium chloride, and sodium. In section IV, we summarize our findings and give an outlook on future work.

II. THEORY AND METHODS

A. Projected Crystal Orbital Hamilton Populations. Let us assume we have succeeded in a self-consistent electronic-structure calculation using a plane-wave basis set with a fine-meshed \mathbf{k} -point set in reciprocal space to comply with Bloch’s theorem. As a result, we obtain the band functions $\psi_j(\mathbf{k}, \mathbf{r})$ in which j denotes the band number, and any given band function may be expressed as

$$\psi_j(\mathbf{k}, \mathbf{r}) = \sum_{\mathbf{G}} C_{j\mathbf{G}}(\mathbf{k}) \exp\{i(\mathbf{k} + \mathbf{G}) \cdot \mathbf{r}\} \quad (1)$$

At first sight, these band functions are just a mathematical construct, namely a linear combination of plane waves using reciprocal lattice vectors \mathbf{G} and expansion coefficients $C_{j\mathbf{G}}(\mathbf{k})$. Such an expansion, however, describes the system’s electronic structure as accurately as a linear combination of atomic orbitals (LCAO) would have done. In other words: the LCAO wave functions and the band functions $\psi_j(\mathbf{k}, \mathbf{r})$ must closely resemble each other, despite their grossly different origin. We write down such a \mathbf{k} -dependent LCAO function $\Phi_j(\mathbf{k}, \mathbf{r})$ for the j th band by combining atom-centered, orthonormal one-electron functions (orbitals) $\phi_\mu(\mathbf{r})$ with coefficients $c_{j\mu}(\mathbf{k})$:

$$\Phi_j(\mathbf{k}, \mathbf{r}) = c_{j\mu}(\mathbf{k}) \phi_\mu(\mathbf{r}) + c_{j\nu}(\mathbf{k}) \phi_\nu(\mathbf{r}) + \dots \approx \psi_j(\mathbf{k}, \mathbf{r}) \quad (2)$$

Figure 1 exemplifies both expansions from a band function $|\psi_j\rangle$ obtained in a periodic plane-wave calculation for the carbon

monoxide molecule, CO, looking along the C–O direction. The alert chemist will realize that $|\psi_j\rangle$ resembles the 3σ molecular orbital and is composed mainly of a carbon 2s atomic orbital.¹¹ Thus, the band function’s overlap with a local, true s orbital $|\phi_1\rangle$ will be significant for reasons of symmetry while it is exactly zero with respect to a p orbital $|\phi_2\rangle$ because both are perpendicular to each other.

We stress that the choice of localized orbitals $\{|\phi_\mu\rangle\}$ is, in principle, arbitrary⁹ or, more positively expressed, a matter of chemical choice. This is delightful, because we may employ any basis set that is well-suited to our respective chemical question; one might choose, for example, orbitals of the well-known Slater type. Nonetheless, we still need to quantify how well any basis set allows us to simulate the plane-wave band functions $|\psi_j(\mathbf{k})\rangle$. Therefore, we calculate the overlap matrix between the band functions and the local orbitals $|\phi_\mu\rangle$; for reasons that will become clear in the sequel, we name it the “transfer matrix” $\mathbf{T}(\mathbf{k})$, and its elements are given as

$$T_{j\mu}(\mathbf{k}) = \langle \psi_j(\mathbf{k}) | \phi_\mu \rangle \quad (3)$$

Within the LCAO paradigm, we would extract the chemical information directly from the atomic orbital coefficients c_μ and multiplying two coefficients c_μ and c_ν yields the density-matrix element $P_{\mu\nu}$. Similarly, when using plane waves, the analogous information is stored in the transfer matrix. We may thus calculate a projected density matrix $\mathbf{P}^{(\text{proj})}$ for every band j and every \mathbf{k} point, and its elements are

$$P_{\mu\nu}^{(\text{proj})}(\mathbf{k}) = T_{j\mu}^*(\mathbf{k}) T_{j\nu}(\mathbf{k}) \quad (4)$$

Finally, to implement a COHP-like technique, we need to retrieve the Hamiltonian matrix elements $H_{\mu\nu}(\mathbf{k})$ expressed in the basis of the local functions. We do this by using the formulation of ref 9, and then the plane-wave Hamiltonian $\hat{H}^{(\text{PW})}$ expanded in the framework of a complete basis is

$$\begin{aligned} H_{\mu\nu}^{(\text{proj})}(\mathbf{k}) &= \langle \phi_\mu | \hat{H}^{(\text{PW})} | \phi_\nu \rangle \\ &= \sum_j \langle \phi_\mu | \psi_j(\mathbf{k}) \rangle \varepsilon_j(\mathbf{k}) \langle \psi_j(\mathbf{k}) | \phi_\nu \rangle \end{aligned} \quad (5)$$

which is simply

$$H_{\mu\nu}^{(\text{proj})}(\mathbf{k}) = \sum_j \varepsilon_j(\mathbf{k}) T_{j\mu}^*(\mathbf{k}) T_{j\nu}(\mathbf{k}) \quad (6)$$

We now have both matrices available, transferred from a plane-wave to an orbital picture, and we may construct an analogue to the traditional COHP, which we call the “projected crystal orbital Hamilton population” (pCOHP) from now on:

$$\begin{aligned} \text{pCOHP}_{\mu\nu}(E, \mathbf{k}) &= \sum_j \mathcal{N} [P_{\mu\nu}^{(\text{proj})}(\mathbf{k}) H_{\nu\mu}^{(\text{proj})}(\mathbf{k})] \\ &\quad \times \delta(\varepsilon_j(\mathbf{k}) - E) \end{aligned} \quad (7)$$

Note that the above expression is energy-dependent because a delta function ensures that the density matrix only has nonzero entries at the specific band energy $\varepsilon_j(\mathbf{k})$; alternatively expressed, the density matrix has been rewritten into a density-of-states matrix. To obtain the real-space pCOHP(E), the sum over all orbitals μ (centered at the first atom involved in the bond in question) and ν (at the second atom) is calculated, and a subsequent \mathbf{k} -space integration is performed; technically, the latter is most

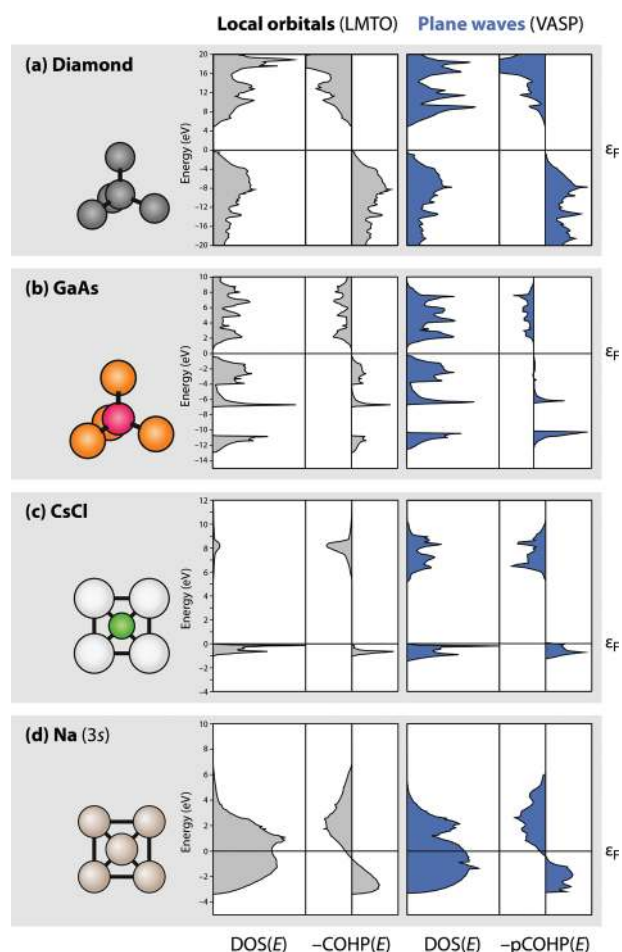


Figure 2. Density-of-states (DOS) and crystal orbital Hamilton population (COHP) analysis for the nearest-neighbor interactions in (a) diamond, (b) GaAs, (c) CsCl, and (d) Na, showing “traditional” calculations based on atom-centered LMTOs (left) and plane-wave calculations using the newly introduced pCOHP method (right). DOS are given in states per electronvolt and cell, and COHP/pCOHP are given per cell. All energies are shown relative to the Fermi level ϵ_F .

efficiently done by using the tetrahedron method proposed by Andersen¹² and improved by Blöchl.¹³

B. Computational Details. Plane-wave electronic structure calculations were performed using density-functional theory (DFT) in the generalized gradient approximation (GGA) as parametrized by Perdew, Burke, and Ernzerhof.¹⁴ The Vienna ab initio Simulation Package (VASP),¹⁵ version 4.6, was used, employing the usual means of modeling the core states, namely, Blöchl’s projector-augmented wave (PAW) method¹⁶ for diamond, GaAs, and Na, and ultrasoft pseudopotentials of the Vanderbilt type¹⁷ for CsCl. Sets of \mathbf{k} points were selected according to the Monkhorst–Pack scheme,¹⁸ and careful checks were made for convergence with respect to the \mathbf{k} -point mesh and cutoff energy, the latter being 400 eV for diamond, 209 eV for GaAs, 274 eV for CsCl, and 127.5 eV for Na. Cell parameters were allowed to relax (resulting in $a = 2.503$ Å for the primitive unit cell of diamond, $a = 4.071$ Å for that of cubic GaAs, $a = 3.962$ Å for CsCl, and $a = 4.187$ Å for Na) with a convergence criterion of $\Delta E \leq 10^{-5}$ eV. Electronic structures were optimized until residual energetic changes were smaller than 10^{-7} eV.

For the pCOHP projection technique, the transfer matrix elements were calculated using a VASP-internal subroutine and

taken from the resulting output file. Local functions (centered at the respective atomic positions \mathbf{R}_A) were constructed within VASP using Bessel functions^{15,19} as a simple orbital substitute in the range of $|\mathbf{r} - \mathbf{R}_A| \leq R_{WS}$ and assuming zero value outside the Wigner–Seitz spheres. The Wigner–Seitz radii were set to $R_{WS}(\text{C}) = 0.863$ Å, $R_{WS}(\text{Ga}) = 1.402$ Å, $R_{WS}(\text{As}) = 1.217$ Å, $R_{WS}(\text{Cs}) = 2.831$ Å, $R_{WS}(\text{Cl}) = 1.111$ Å, and $R_{WS}(\text{Na}) = 1.757$ Å, as recommended by the VASP manual.²⁰ A minimal basis of one s-like, three p-like, and (for GaAs and CsCl) five d-like functions was used for projection. A custom program²¹ was employed to read these projection values from the VASP output and subsequently calculate projected density-of-states matrices (implementing eq 4), Hamiltonian matrices (eq 5), and the projected COHP (eq 7). Integration in reciprocal space was finally performed using the tetrahedron method as described above, to arrive at an energy-resolved pCOHP(E) plot.

For a comparison with the traditional, direct COHP method, we also performed linear muffin-tin orbital (LMTO) calculations with the all-electron, quasi-relativistic tight-binding LMTO program in the atomic spheres approximation (TB-LMTO-ASA, version 4.7),²² employing the local density approximation (LDA) as tabulated by von Barth and Hedin.²³ Optimized cell parameters were taken from the VASP calculations. DOS and COHP plots were finally generated using the wxDragon²⁴ visualization tool.

III. APPLICATION

A. Diamond. Diamond is both a simple and well-suitable model substance for our first projected COHP. As described above, electronic-structure calculations were performed with the VASP and also LMTO packages for arriving at self-consistent DFT ground states.

Figure 2a shows the resulting plane-wave DOS and pCOHP(E) plots side by side together with, for reasons of comparison, the traditional DOS and COHP plots that rely on short-ranged, atomic-like LMTOs. We stick to the usual way of displaying COHPs, namely drawing negative (i.e., bonding) contributions to the right and positive (i.e., antibonding) to the left, and we remind the reader that integrated COHPs are pairwise contributions to an effective one-particle energy, the so-called band-structure energy. We also stress that all interpretation of chemical bonding given here is qualitative, and we deliberately do not add a scale to the horizontal axis because we consider it of no additional value, at least at the present time.

As seen from the DOS plots, both LMTO and VASP arrive at essentially superimposable valence bands, despite the extremely different basis sets and, also, the somewhat differing exchange–correlation functionals, just as expected. With respect to the chemical bonding, all valence states (below the Fermi level ϵ_F) appear as bonding while antibonding states (above ϵ_F) are detected solely in the conduction bands. This result is equally found for the projected COHP and the traditional COHP. Also, the shapes of the valence and conduction bands, in particular no energetic separation whatsoever between the 2s and 2p orbitals, indicate very strong orbital mixing (“hybridization”), quite typical for elemental carbon because of the similar spatial extent of 2s and 2p.

There are also some VASP/LMTO differences, however, in particular within the unoccupied bands where both DOS plots begin to differ in shape, but this is unimportant for the chemical bonding. More subtle differences are found by comparing COHP and pCOHP below the Fermi level, despite the fact that all

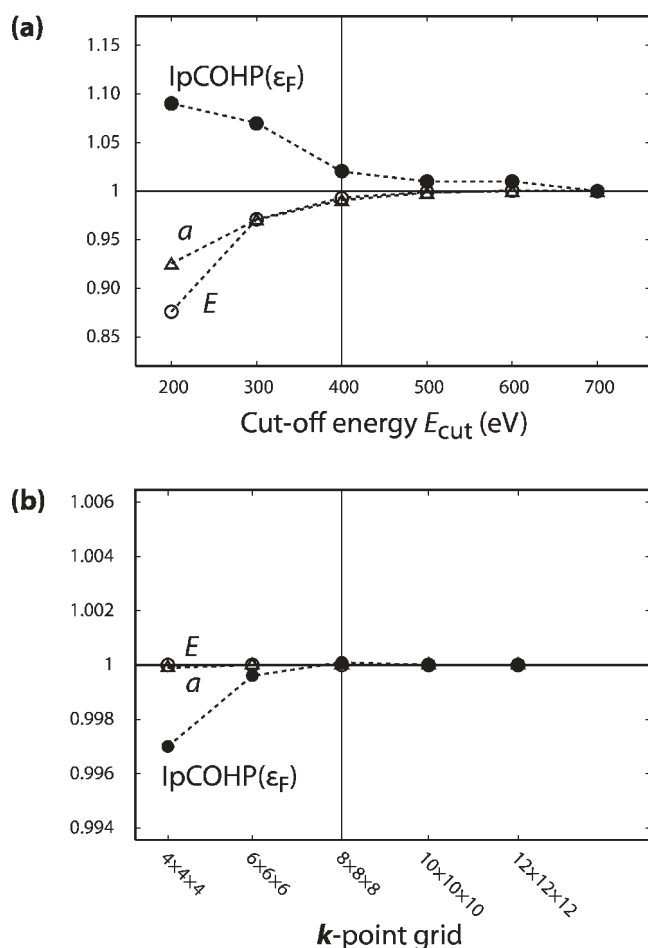


Figure 3. Convergence of results with respect to (a) cutoff energy and (b) k point grid according to the Monkhorst–Pack scheme. Predicted total energies E (open circles), cell parameters a (triangles), and integrated pCOHP at the Fermi level ϵ_F (filled circles) have been normalized to unity, respectively. Parameters used for the pCOHP analysis as shown in Figure 2 are indicated by a vertical line.

essential chemical information (that is, the pCOHP *shape* showing bonding and antibonding interactions) is correctly reproduced. Also, we stress that the traditional COHP, which relies on a highly specialized local basis set, should not be looked upon as a kind of standard that needs to be perfectly imitated by the plane-wave derived pCOHP.

Before moving on to the next example, let us discuss one more technical point, namely, the convergence of results with respect to the basis-set size (as controlled by the cutoff energy E_{cut}) and the density of the k-point mesh. Commonly, one ensures this convergence by increasing both parameters until the predicted total electronic energy E or lattice parameter a no longer differs from the prior result. Here, we investigate this behavior for the pCOHP as well. It is convenient to compare the *integrated* values of the projected COHP; the latter is defined, in analogy to the traditional integrated COHP (ICOHP), by calculating the energy integral up to the highest occupied bands:

$$\text{IpCOHP}(\epsilon_F) = \int^{\epsilon_F} \text{pCOHP}(E) dE \quad (8)$$

All three quantities (energy, lattice parameter, integrated pCOHP) were calculated using various values of both cutoff

energies and number of k points N_k , and then they were plotted using a normalized scale, for simple reasons of convenience. Figure 3 displays the results. Upon increasing the plane-wave basis set (i.e., the cutoff energy), the integrated pCOHP values converge smoothly, in a way comparable to the behavior of the other two quantities. To put it simply, a pCOHP analysis requires no larger basis set than the preceding electronic-structure calculation does. With respect to k point grid size, the convergence behavior displayed in Figure 3 is quite comparable. Using a rather compact $8 \times 8 \times 8$ Monkhorst–Pack grid, as is common for calculations on diamond, neither energy nor pCOHP deviate by more than 0.01% when compared to a more costly $12 \times 12 \times 12$ grid. These are perfectly acceptable results in terms of convergence.

B. Gallium Arsenide. In going from diamond to the almost isotypical GaAs crystal, the problem gets slightly more sophisticated: first, the larger number of orbitals will end up in a more complicated electronic structure. Second, different species of atoms are involved; thus the difference of electronegativities introduces a (small) electrostatic contribution.

The two DOS figures in Figure 2b, again, indicate almost superimposable electronic structures, in particular concerning the valence region, despite the very different basis sets and differing exchange–correlation functionals. Somewhat simplified, the valence region is almost entirely composed of arsenic 4s (around -12 eV) and 4p bands (between -7 eV and the Fermi level), and the internal gap (at around -9 eV) reflects the weaker mixing between 4s and 4p orbitals.

Figure 2b also shows the results of the Hamilton population analysis using both traditional and projected COHP approach. Once again, the crystal’s chemical bonding is well described, and the entire valence band results as being bonding. Nonetheless, a small weakness is obvious from the pCOHP plot: while the energetically lowest (4s) levels are seemingly overestimated in their bonding character as compared to the traditional COHP’s prediction, the higher-lying with mostly 4p character (in particular those close to ϵ_F) are underestimated. An explanation is fairly obvious, at least qualitatively. Just like in the first COHP publication,² the projection routine has been limited to a minimal basis, that is, one s, three p, and five d orbitals for GaAs, and we expect improved results for a larger basis. The aforementioned problem becomes even more serious when choosing simple Bessel functions (readily available in VASP) as a primitive replacement of real atomic orbitals; in comparison, the traditional COHP method uses density and Hamiltonian matrix elements *directly* obtained from the highly specialized localized muffin-tin orbitals. In addition, the projection is performed using identical Wigner–Seitz spheres for all orbitals of a given atomic species, and this does not comply with the grossly different spatial extent of these atomic orbitals, in particular 4s and 4p; finally, the formal requirement of nonoverlapping Wigner–Seitz spheres is absent in the LMTO calculations used here. To name but an example, a larger Wigner–Seitz radius for arsenic ($R_{\text{WS}}(\text{As}) = 1.447 \text{ \AA}$) was employed by the TB-LMTO-ASA program, as compared to $R_{\text{WS}}(\text{As}) = 1.217 \text{ \AA}$ in our projection technique. Further studies are currently being undertaken to optimize the basis functions used for projection, assessing, e.g., well-fitting linear combinations of Slater-type orbitals.

C. Cesium Chloride. Cesium chloride may seem a surprising subject, because the concepts presented here refer to our typical notion of covalent bonding through orbital interactions. Let us, nonetheless, treat a paradigmatically ionic crystal with the methods developed so far.

As a rule of thumb, the more localized the bonding electrons, the narrower and “simpler” the bands.²⁵ The VASP- and LMTO-derived densities-of-states are plotted in Figure 2c and, not too surprisingly, they do look very simple and consist of one area right below ϵ_F and one above, at 8 ± 2 eV, in the virtual bands. A moment reflection or a partial DOS analysis (not shown) reveals that the valence area is almost completely composed of filled chlorine 3p bands while the conduction band is just the unoccupied cesium 6s level. Note that the more localized basis set (LMTO) also leads to a more localized description of the material if compared to the VASP result: within the filled bands, both DOS shapes look alike although VASP tends toward slightly larger delocalization. Coming back to the chemical bonding looked at with an orbital tool, even the classical electrostatic notion (one electron jumping from Cs to Cl) is recovered because it is favorable to have electron density at the chlorine anion (where the states have bonding character, and are filled), but not at the cesium cation. Thus, COHP and also pCOHP analysis describe the bonding in CsCl efficiently, justifying its use on bonds with strong electronegativity differences. While cesium chloride itself is not a thrilling subject, there are many “ionic” solids that are.

D. Sodium: The Other Extreme. We have started our discussion with typical covalent solids and have moved on to a highly ionic substance. To round out the picture, we finally discuss a clearly metallic system, namely, crystalline sodium, and limit ourselves to a description of the 3s orbital actively involved in what a chemist or physicist defines as “metallic bonding”. Figure 2d contrasts LMTO calculations (obtained by downfolding the 3p states, as described in detail in ref 26) with our plane-wave technique. As is clearly visible, the COHP shows pairwise interactions in an occupied (bonding) and an unoccupied (antibonding) band. Note that the density-of-states closely resembles what is to be expected for a free electron gas,²⁷ consistent with the notion of completely “delocalized bonds” in metals. The DOS obtained from VASP (for direct comparability with LMTO, we only show the 3s contributions) looks qualitatively alike and so does the projected COHP analysis. We have thus exemplified that all three “classical” concepts of bonding in solids—covalent, ionic, and metallic—can be correctly described not only by the traditional but also by the projected COHP technique. Of course, there exists only *one* electronic structure that we humans interpret in different ways.

IV. CONCLUSIONS

In this paper, we have shown how to derive an energy-resolved local bonding analysis based on the results of plane-wave electronic-structure calculations, defined as “projected crystal orbital Hamilton population” (pCOHP). Starting from any given atom-centered, orthonormal basis set $\{|\phi_{\mu}\rangle\}$, both the density matrix $\mathbf{P}(\mathbf{k})$ and Hamiltonian matrix $\mathbf{H}(\mathbf{k})$ can be reconstructed using properly calculated transfer matrices that refer to such a basis. Once both matrices are known, the calculation of a COHP analogue is straightforward. Thus, it is no longer necessary to calculate the band functions using specialized local orbitals (as in the TB-LMTO-ASA or the extended Hückel methods which are, so far, the only ways of performing a COHP analysis), but one may stick to fast and efficient electronic-structure calculations with any plane-wave program of choice. Then follows the projection technique, which demands orders of magnitude less computational power.⁹ Even a crude approximation for the local basis such as Bessel functions, which is the only one available in this

context so far, provides a chemically correct interpretation of the crystals’ bonding.

The feasibility of the pCOHP method has been demonstrated using four textbook examples, and all chemical information as exemplified by the traditional COHP analysis has been recovered. The advantage of the new pCOHP approach, however, will be obvious from more complex materials, in particular those that can no longer be considered as being close-packed: chemical bonding studies in absorption, surface processes, and low-dimensional materials that pose enormous difficulties for tight-binding LMTO-ASA but not at all for plane-wave approaches.

Remaining, more technical problems deal with the optimization of the sort and spatial extent of the local orbitals to be used for projection. Additionally, we are currently designing a versatile program that will not only calculate the projection values independent of VASP but will also be compatible with a multitude of available plane-wave codes. This, together with more complex chemical studies, will be the subject of a forthcoming publication.

AUTHOR INFORMATION

Corresponding Author

*Electronic mail: drons@HAL9000.ac.rwth-aachen.de.

ACKNOWLEDGMENT

V.L.D. gratefully acknowledges a scholarship from the German National Academic Foundation. A.L.T. acknowledges support by the Russian Foundation for Basic Research.

REFERENCES

- (1) Hoffmann, R. *Solids and Surfaces. A Chemist's View of Bonding in Extended Structures*; VCH: Weinheim and New York, 1988.
- (2) Dronskowski, R.; Blöchl, P. E. *J. Phys. Chem.* **1993**, *97*, 8617.
- (3) Hughbanks, T.; Hoffmann, R. *J. Am. Chem. Soc.* **1983**, *105*, 3528.
- (4) Hoffmann, R. *J. Chem. Phys.* **1963**, *39*, 1397. Hoffmann, R. *J. Chem. Phys.* **1964**, *40*, 2745. Hoffmann, R. *J. Chem. Phys.* **1964**, *40*, 2474.
- (5) See, e.g.: Landrum, G. A.; Dronskowski, R. *Angew. Chem., Int. Ed.* **2000**, *39*, 1560. Dronskowski, R.; Korczak, K.; Lueken, H.; Jung, W. *Angew. Chem., Int. Ed.* **2002**, *41*, 2528.
- (6) Bloch, F. *Z. Phys.* **1929**, *52*, 555.
- (7) For a review see, e.g.: Segall, M. D.; Lindan, P. J. D.; Probert, M. J.; Pickard, C. J.; Hasnip, P. J.; Clark, S. J.; Payne, M. C. *J. Phys. Condens. Matter* **2002**, *14*, 2717.
- (8) Hafner, J. *J. Comput. Chem.* **2008**, *29*, 2044.
- (9) Sánchez-Portal, D.; Artacho, E.; Soler, J. M. *Solid State Commun.* **1995**, *95*, 685.
- (10) Segall, M. D.; Shah, R.; Pickard, C. J.; Payne, M. C. *Phys. Rev. B* **1996**, *54*, 16317.
- (11) In contrast to a real 2s orbital, the resulting band function is nodeless, simply due to the very nature of the pseudopotential approach.
- (12) Jepsen, O.; Andersen, O. K. *Solid State Commun.* **1971**, *9*, 1763.
- (13) Blöchl, P.; Jepsen, O.; Andersen, O. K. *Phys. Rev. B* **1994**, *49*, 16223.
- (14) Perdew, J. P.; Burke, K.; Ernzerhof, M. *Phys. Rev. Lett.* **1996**, *77*, 3865.
- (15) Kresse, G.; Hafner, J. *Phys. Rev. B* **1993**, *47*, 558. Kresse, G.; Furthmüller, F. *Comput. Mater. Sci.* **1996**, *6*, 15.
- (16) Blöchl, P. E. *Phys. Rev. B* **1994**, *50*, 17953.
- (17) Vanderbilt, D. *Phys. Rev. B* **1990**, *41*, 7892.
- (18) Monkhorst, H. J.; Pack, J. D. *Phys. Rev. B* **1976**, *13*, 5188.
- (19) For details on Bessel functions, see: Watson, G. N. *A Treatise on the Theory of Bessel Functions*, 2nd ed.; Cambridge University Press: Cambridge, 1944. Olver, F. W. J., Lozier, D. W., Boisvert, R. F., Clark,

C. W., Eds. *NIST Handbook of Mathematical Functions*; Cambridge University Press: Cambridge, U.K., 2010.

(20) The alert reader will immediately recognize that the Wigner–Seitz radii exceed the atomic radii by a small amount; thus, the Wigner–Seitz spheres at neighboring atoms overlap such that the local basis functions are no longer perfectly orthogonal. No qualitative differences in the pCOHP plots occur, however, as has been checked by comparing the results from different Wigner–Seitz radii. We thus keep the values as recommended in the potential file.

(21) Deringer, V. L. *Diploma thesis*, RWTH Aachen University, 2010.

(22) Andersen, O. K. *Phys. Rev. B* **1975**, *12*, 3060. Andersen, O. K.; Jepsen, O. *Phys. Rev. Lett.* **1984**, *53*, 2571.

(23) von Barth, U.; Hedin, L. *J. Phys. C: Solid State Phys.* **1972**, *5*, 1629.

(24) Eck, B. *wxDragon 1.7.1*; RWTH Aachen University: Aachen, Germany, 2010.

(25) Dronskowski, R. *Computational Chemistry of Solid-State Materials*; Wiley-VCH: Weinheim and New York, 2005.

(26) Lambrecht, W. R. L.; Andersen, O. K. *Phys. Rev. B* **1986**, *34*, 2439.

(27) Ashcroft, N. W.; Mermin, N. D. *Solid State Physics*; Holt, Rinehart & Winston: New York, 1976.